Int. J. Electrochem. Sci., 10 **(2015)** 9919 - 9932

International Journal of
ELECTROCHEMICAL
SCIENCE
www.electrochemsci.org

Rapid Corrosion Testing of Polymer Coated Steel Using a Constant Voltage

Junwei Wu[1,*], *Yanhui Cui*[1], *Wei Yuan*[1], *Junsheng Wu*[2], *Zuohua Li*[3]

[1] Shenzhen Key Laboratory of Advanced Materials, Department of Materials Science and Engineering, Harbin Institute of Technology Shenzhen Graduate School, Shenzhen, 518055, China
[2] Institute of Advanced Materials and Technology, University of Science and Technology Beijing, Beijing, 100083, China
[3]School of Civil and Environmental Engineering, Harbin Institute of Technology Shenzhen Graduate School, Shenzhen 518055, China
[*]E-mail: junwei.wu@hitsz.edu.cn

Received: 8 July 2015 / *Accepted:* 2 October 2015 / *Published:* 4 November 2015

An alternative to accelerated corrosion performance evaluation, e.g. neutral salt spray test (NSS), is proposed by applying a constant voltage in a corrosive media. In this work, polyurethane coated steels were tested at 3.5 V in a 3.5% NaCl solution. NSS was done to allow comparison with the constant voltage test. Electrochemical impedance spectroscopy (EIS) tests were carried out periodically to study the corrosion procedures. Generally, it takes just 90 h for constant voltage to reach a similar state as NSS after 20 days, confirming that the acceleration rate of the constant voltage method is significantly more rapid than the established NSS test.

Keywords: polymer coating; electrochemical impedance spectroscopy; neutral salt spray test; constant voltage

1. INTRODUCTION

Polymer coatings have been widely used to enhance the appearance, UV-resistance, mechanical properties, and most importantly, to enhance the corrosion resistance by acting as a barrier layer to separate the substrate metal from its environment [1-4]. However all polymers are permeable to potentially corrosive species such as oxygen, water and ions. The penetration of oxygen and ions may facilitate the oxidation or corrosion rate [4-6], and water molecules at the metal/coating interface may be harmful to the coating adhesion; thus favoring the metal corrosion underneath the coatings [4]. The anti-corrosive performances of coatings typically have a direct relationship with the service life of the

protected parts. Consequently it is critical to have some widely recognized method to evaluate the performance, such as electrochemical impedance spectroscopy, salt spray test, and so on.

EIS is a non-destructive tool useful for examining the corrosion performance of coated metals in aqueous environments [7]. The use of equivalent circuit simulations allows estimated values of the elements in the circuit and these can provide information concerning water uptake in the coating, changes in the resistive properties of the polymer layer(s), development of coating delamination, and initiation and propagation of corrosion at the metal/coating interface [8-11]. Previously EIS had been extensively used to study the corrosion mechanism of a coating and evaluate coating performance. Shreepathi [8] utilized EIS to study the zinc content on the effect of anti-corrosion performance of epoxy zinc rich coatings. Xiong [9] compared different coating systems by EIS to rank the performance. Souto [5] studied the degradation process of polyurethane coating using EIS and showed that a polyurethane coating had higher adhesion and enhanced anticorrosion protection characteristics when applied on carbon steel than was obtained on galvanized steel. Floyd [10] attempted to evaluate the corrosion resistance of coated but unexposed metal panels by EIS, so as to predict the performance of coated panels that were subjected to both continuous and cyclic corrosion testing. Shreepathi [11] compared the actual lifetime of organic coatings with the lifetime predicted by EIS.

NSS is undoubtedly the most common method to rank the relative performance of polymer coatings [12], typically based on a series of ASTM standards [13-15]. Alternative test methods include: immersion test, UV test, and humidity cabinet test [11], but all the above methods typically require long times (500 to 2000 h) to complete the evaluation, which limits their use in industrial applications. Therefore, it is useful to develop a rapid method to evaluate the protective performance, for example: Hall [12] compared the corrosion resistance of coatings by NSS and electrochemical pitting test, which verified that the later one is reliable if pitting is the main issue. Appleman [16] used a "stress environment" for accelerating coatings failure which included immersion in an electrolyte, placed in a continuous salt fog at 35 ^{o}C, a SO_2 salt fog, and cyclic salt fog; Tobiszewski [17] tried to assess anti-corrosive coatings more effectively by using "electrochemical noise"; Bierwagen [18] proposed a new accelerated evaluation method of "thermal cycling testing", including 3 days of heating/cooling during immersion followed by 3 days of room temperature immersion.

In this work an alternative accelerated corrosion performance evaluation method is proposed by using a constant voltage test. The constant voltage facilitates the permeation of corrosive species throughout the polymer coatings which promotes the corrosion process. In order to allow for comparison, a NSS test was also conducted. EIS was used to measure the corrosion processes in both the constant voltage and the NSS test. Here the coating system of Galvanized steel /Epoxy zinc-rich primer (ZRP) /Polyurethane was chosen because it is the most popular one for outdoor applications.

2. EXPERIMENTAL

2.1 Coating preparation

Galvanized mild carbon steel plates (0.12% C; 0.50% Si; 0.60% Mn; 0.10% P; 0.045% S, 0.30% Ti, in mass%) were used as substrates with the measuring size of 150 ×80 ×1 (mm), and the

zinc coating was 5~8 μm thick. Prior to coating, the plates were cleaned by immersion for 1 min in a bath containing a proprietary alkaline solution assisted by ultrasonic agitation, then rinsed with deionized water couples of times right before the coating process.

The powder coating is consisting of two layers: a primer layer of ZRP with Zn content no less than 40%, and a top layer of polyurethane. Both of them were applied to the cleaned galvanized surfaces using a Wagner PEM-X1 electrostatic spray gun. All the powders are supplied from Akzonobel (Shenzhen branch, China), Interpon PZ 660 for the ZRP sublayer and Interpon 600 for the top layer. After ZRP coating, the samples were then placed in an oven for about 15 min at 180 ^{o}C to cure before applying the top layer. Then the top polyurethane layer was cured 15 min at 200 ^{o}C in oven to finish the coating process. The entire processes were finished by Shenzhen ZTE Holdings Co., Ltd. Coating specifications are summarized in Table 1.

Table 1. Coating specifications

	Powders	Name	Thickness	Curing
Substrate	--	Galvanized steel	5-8μm (Zn coating)	
Primer	Interpon PZ 660	Epoxy zinc-rich primer (ZRP)	24-30μm	180 ^{o}C, 15 min
Top coating	Interpon 600	Polyurethane	120-130μm	200 ^{o}C, 15 min

2.2 Accelerated constant voltage and NSS test

Accelerated constant voltage test was conducted in 3.5 wt.% NaCl (CR grade, Tianjin Yongda Chemical) solution at room temperature with 3.5 V applied to the work pieces by CHI 760D electrochemical workstation (CH Instruments, Shanghai, CHINA). The counter and reference electrode were connected together to a graphite electrode with the same dimension as the specimens. The distance between anode and cathode was set as 90 mm. In order to avoid any edge effects, all the edges of each specimen were sealed by wax.

The NSS tests were conducted according to ASTM B117, testing 5 parallel plates simultaneously. Visual examination was used to determine the extent of corrosion damage, which was categorized as “white rust” and “red rust”, representing corrosion of the zinc and the underlying steel, respectively.

2.3 EIS test

Electrochemical measurements were measured with a CHI760D workstation with a three-electrode system. The polymer coated sample acted as the working electrode with an exposed surface area of 3 cm^2, an Ag/AgCl (saturated KCl) electrode was used as the reference electrode, and a

graphite plate as the counter electrode. The electrolyte used was a 3.5 wt.% NaCl solution with the pH of 6.7. The impedance measurement was conducted in the frequency range of 100 kHz to 1 mHz by applying an AC voltage with an amplitude of 10 mV around the open circuit potential. The system was stabilized for 30 min before EIS measurement. Each experiment was done using 5 parallel samples and the most representative ones were chosen as the results. All the EIS experimental data was analyzed with ZSimpWin software.

2.4 Material Characterizations

The surface morphology of the coating and the corrosion product of the surface was analyzed by scanning electron microscopy (SEM, Hitachi S3400) and energy dispersive spectrometer (EDS, Oxford Instruments), with the accelerating voltage of 15kV.

3. RESULTS

3.1 Visual examination

The coating is dense and uniform and each layer is well adhered to its adjacent layer. During the constant voltage test, no gas bubbles were observed initially, but within a few hours small bubbles appeared on the surface of the specimens which implies the beginning of corrosion reactions. Since, during potentiostatic polarization of a polymer coated metal, the potential drop across the polymeric coating layer is several orders of magnitude larger than that across the metal/polymer interface. Consequently it will take some time for the conductive species to permeate through the coating to initiate reaction [4] and after 90 h, red rust was observed on the surface confirming corrosion of the steel. However, in the case of the NSS test, the coating surface remains almost unchanged before white rust was observed after 20 d, then red rust appeared after 22 d. It is noted that no white rust was observed before red rust appeared (90 h) for constant voltage test, which may be due to the zinc corrosion product being dissolved into the solution.

3.2 Surface characterization of red rust

Optical and SEM images of the constant voltage and NSS tested samples are shown in Figure 1. The red rust, that appears on the surface of the constant voltage test samples after 90 h, is shown in Figure 1 (a), (b) and (c). There is an area of the coating ~0.5 mm that is raised with a crack at the perimeter and EDS analysis (Figure 1 (d)) shows that Fe, Zn, C, O, with the Fe:Zn ratio = 16:1 (at.%), which suggests both Fe and Zn have been oxidized. In previous literature, the corrosion products of Zn may include ZnO [5, 19-20], $Zn(OH)_2$ [21], $Zn(HCO_3)_2$ [22,23], $ZnCO_3$ [24] and $3Zn(OH)_2 \cdot 3ZnCO_3$ [25-26]. Figure1 (e), (f) and (g) show the surface morphology of the “red rust” spot after NSS test. As seen in Figure 1(f) it is smaller and less rounded than seen for the constant voltage sample (Figure 1(b)). Figure 1(g) shows there are also micro-sized particles uniformly dispersed on the rust surface.

EDS analysis of this area (Figure 1 (h)) shows the same elements (Fe, Zn, C, O) with the same Fe:Zn ratio (16:1) as detected for the constant voltage sample.

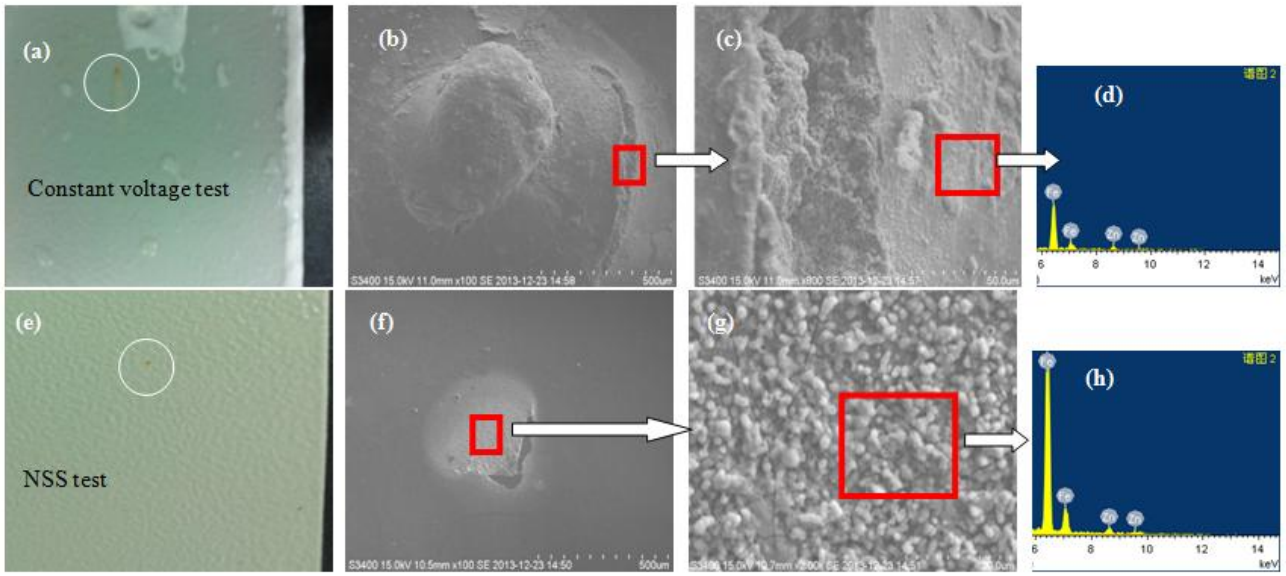

Figure 1. Analysis of "red rust" after constant voltage [(a), (b) (c) and (d)] and NSS test [(e), (f), (g) and (h)]. (a), (e):overview of specimens; (b), (f): Low magnification morphology by SEM; (c), (g): High magnification morphology by SEM for the marked area in (b) and (f), respectively; (d),(f): EDS analysis in marked area of (c), (g), respectively.

3.3 Current variation during constant voltage test

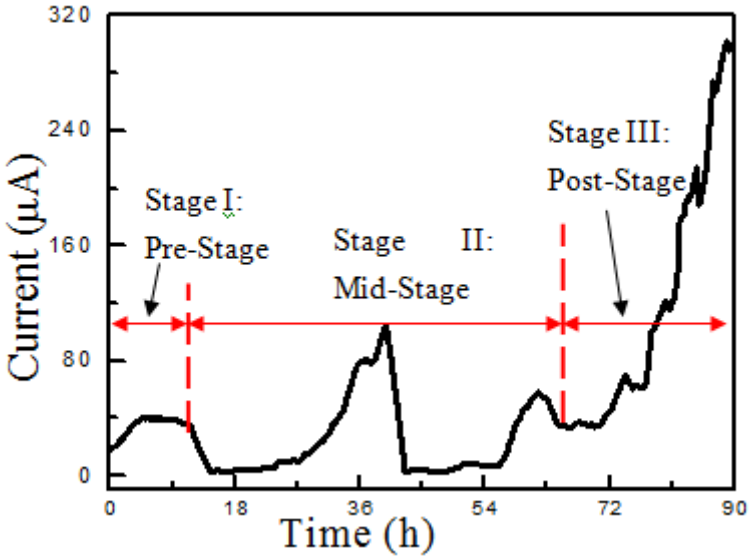

Figure 2. Dependence of monitored current on test time with an applied constant voltage of 3.5 V vs. graphite ($V_{Graphite}$ = 0.226 V vs. SCE)

Figure 2 shows the current variation, with elapsed time, during constant voltage testing. It is observed that there are three separate stages and these are labeled: pre-stage (0-11 h), mid-stage (11-70 h), and post-stage (after 70 h). In the pre-stage the current gradually increases to a plateau and remains stable for approximately 11 hours, and then falls away. In the mid-stage, the current rises to a higher level than measured in the pre-stage and then falls to the minimum after about 40 h and then increases again after 60h, before falling away to a current level similar to that reached in the pre-stage (~ 0.5 x 10^{-4} A). After testing for 70 h, the post-stage begins where current increases exponentially, implying vigorous corrosion of the substrate. The current gradually increased until the coating is completely destroyed.

3.4 EIS for constant voltage test

The impedance of all specimens was measured in 3.5% NaCl after 1, 4, 8, 14, 20, 50, 70, 80, 88 and 90 hours. The Nyquist plots obtained are shown in Figure 3 (a) and (b). As seen, the Nyquist plots initially feature a typical single-capacitive semi-circle arc, which represent an electrochemical process with only one time constant. The arc size varies with the time elapsed. From 0 to 8 h, the arc decreases in size, and at 14 h, increases to an even larger arc than the one at 0 h. The arc size then fluctuates between smaller at 20 and 50 h and larger again at 70 h. The Nyquist plots retain the features of single time constant between 0 and 70 h but, as seen in Figure 3(b), after 80 h a 2nd arc appears which is attributed to substrate corrosion.

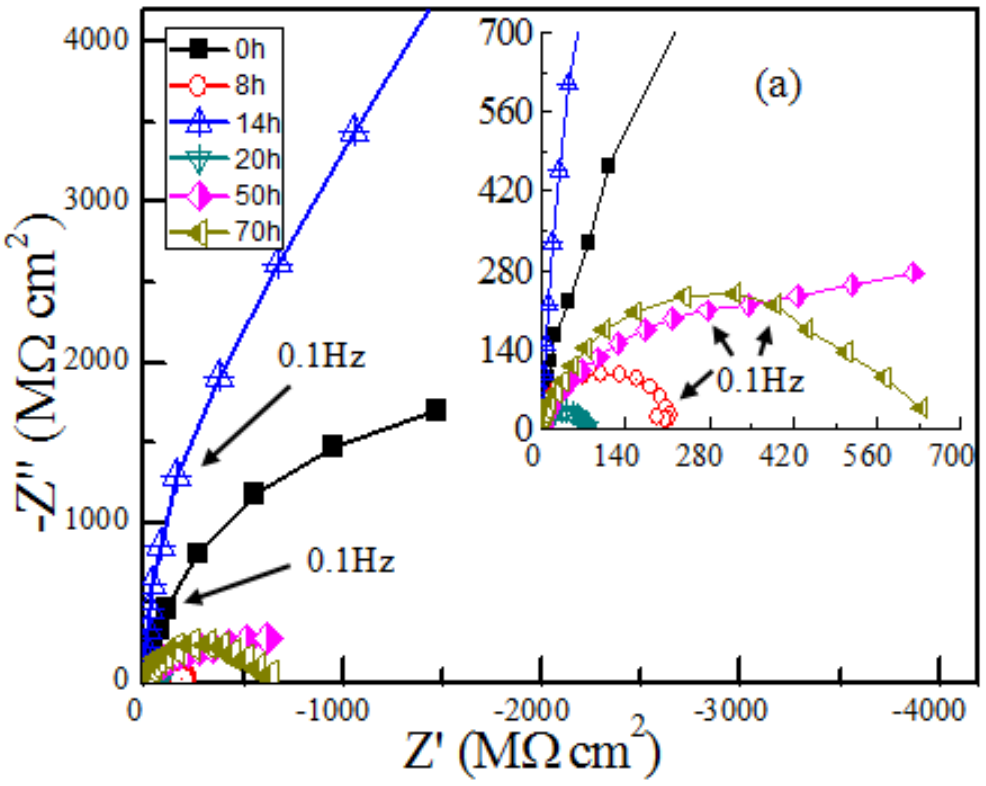

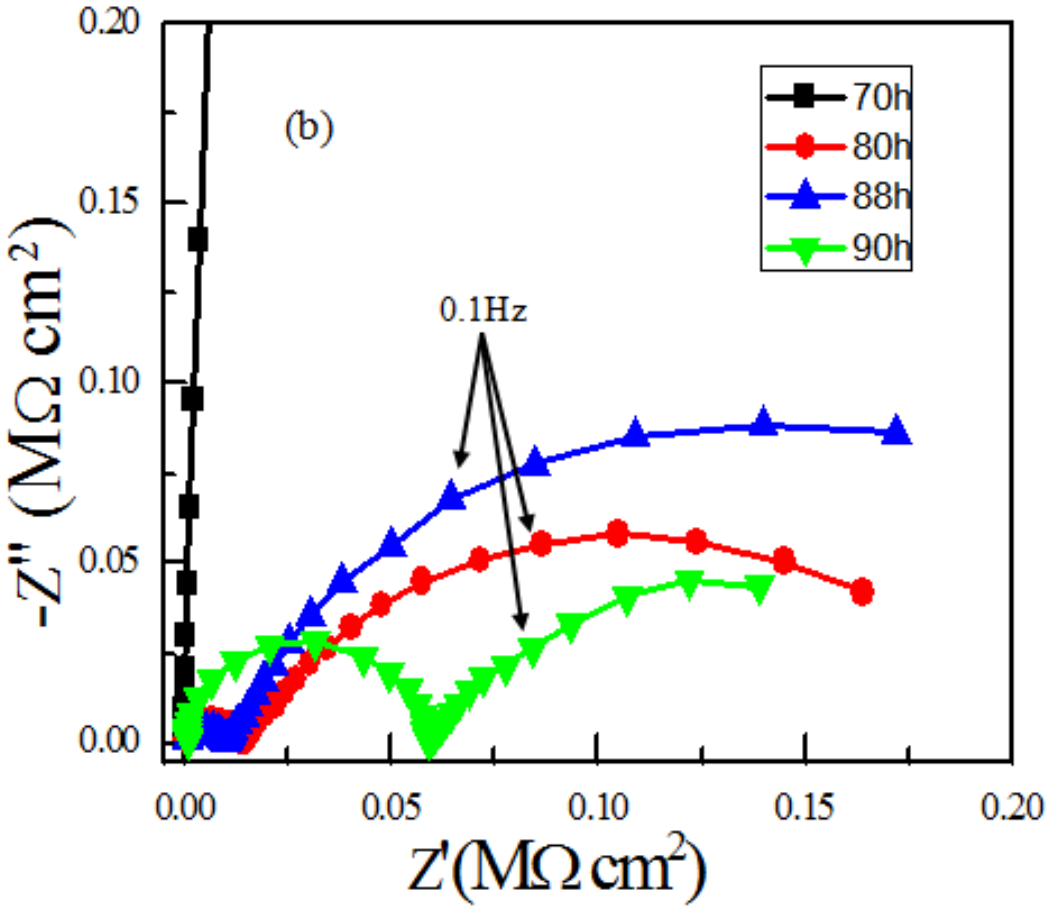

Figure 3. Nyquist plots for coated plates after constant voltage test (a) before 70h, (b) after 70h.

The fitting of EIS data (from 0 to 70 h) was done using a simple equivalent electric circuit model (shown in Figure 4(a)), which is typically used for bare and well coated samples [4,7]. The following elements are incorporated in the model; a resistor R_s (related to resistance of the solution), R_c (the resistance of the organic coating layer), and $CPE_{coating}$ (the constant-phase element used to replace C_p: the organic coating capacitance). This equivalent circuit is extended, as shown in Figure 4(b), to include R_{ct} (the charge transfer resistance of the coated substrate), and CPE_{DL} (the constant-phase element used to replace C_d, the double layer capacitance) to allow fitting of the arcs at 80, 88 and 90 h.

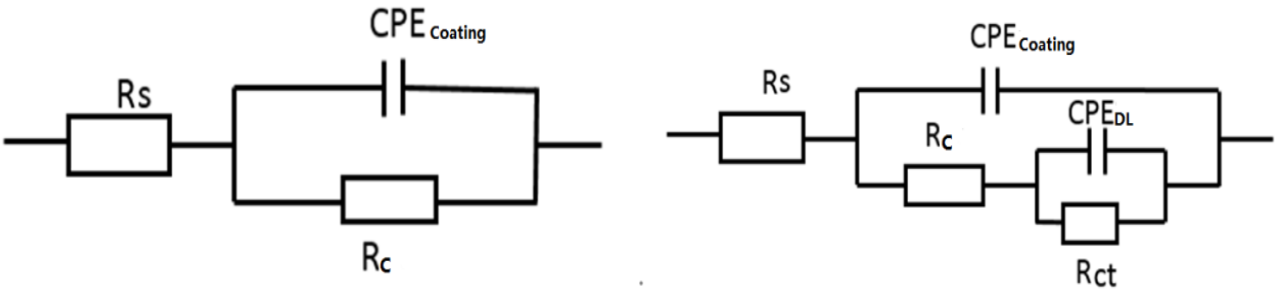

Figure 4. Equivalent circuit model for EIS data simulation.

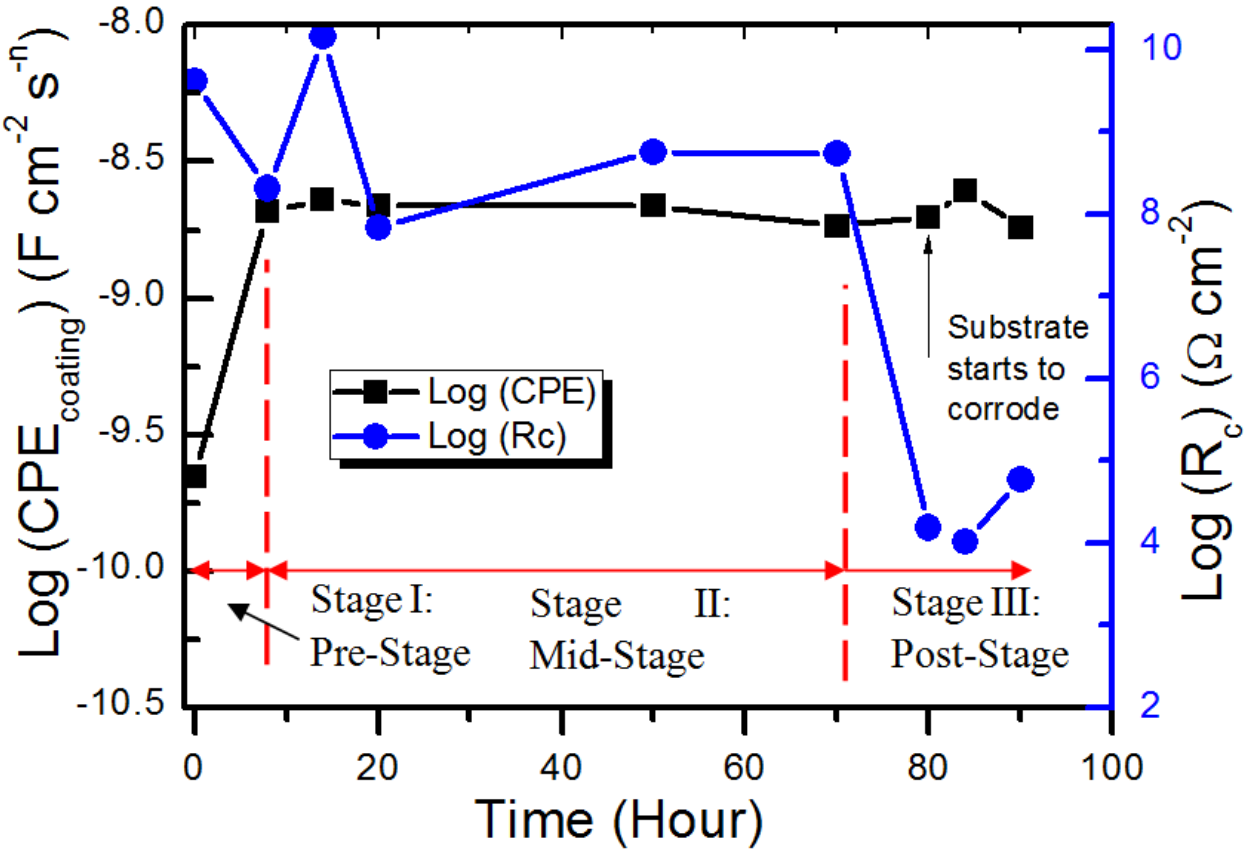

Figure 5. Time dependence of logarithm resistance $CPE_{coating}$ and R_c of constant voltage test.

Table 2. EIS data simulation after constant voltage test

Time (hour)	$CPE_{coating}$ (F cm^{-2} s^{-n})	R_c (Ω cm^{-2})	CPE_{DL} (F cm^{-2} s^{-n})	R_{ct} (Ω cm^{-2})
0	2.218×10^{-10}	4.169×10^{9}	/	/
8	2.078×10^{-9}	2.073×10^{8}	/	/
14	2.298×10^{-9}	1.452×10^{10}	/	/
20	2.187×10^{-9}	6.906×10^{7}	/	/
50	2.169×10^{-9}	5.705×10^{8}	/	/
70	1.841×10^{-9}	5.399×10^{8}	/	/
80	1.975×10^{-9}	1.544×10^{4}	1.247×10^{-5}	1.227×10^{5}
88	2.467×10^{-9}	1.04×10^{4}	2.021×10^{-5}	1.617×10^{5}
90	1.82×10^{-9}	5.99×10^{4}	7.409×10^{-5}	8.477×10^{4}

Based on the equivalent circuits from Figure 4, the exact value of each element can be obtained and these are summarized in Table 2. The logarithm $CPE_{coating}$ and R_c are plotted as a function of test time, as shown in Figure 5. As can be seen the value of $CPE_{coating}$ increases significantly in the pre-stage, due to water adsorption into the coating, and then remains relatively stable during the rest of

constant voltage test. The value of R_c shows a decrease after 8 h (i.e. in the pre-stage region) indicating diffusion of corrosive species, e.g. Cl^-, H_2O into the pores of coating. The value of R_c then reaches a maximum of 1.45×10^{10} Ω cm^{-2} at 14 h before decreasing to its lowest value of 6.91×10^{7} Ω cm^{-2}. The rapid increase in R_c results from the rapid corrosion of ZRP layer and the following decrease is because the pores for diffusion become blocked by the corrosion products of Zn. The fluctuating values of R_c in the mid-stage (from 14 to 70 h) suggests the dynamic self-healing process [27] and the barrier property of the zinc primer coating is functioning. However, as seen in the post-stage (after 80 h), there is a sharp drop in the value of R_c indicating the onset of substrate corrosion and the protection of coating is no longer effective. It is noted that the variation trend of R_c is nearly the opposite trend as the monitored current (see Figure 2), and can also be divided into the same three stages.

3.5 EIS test for NSS test

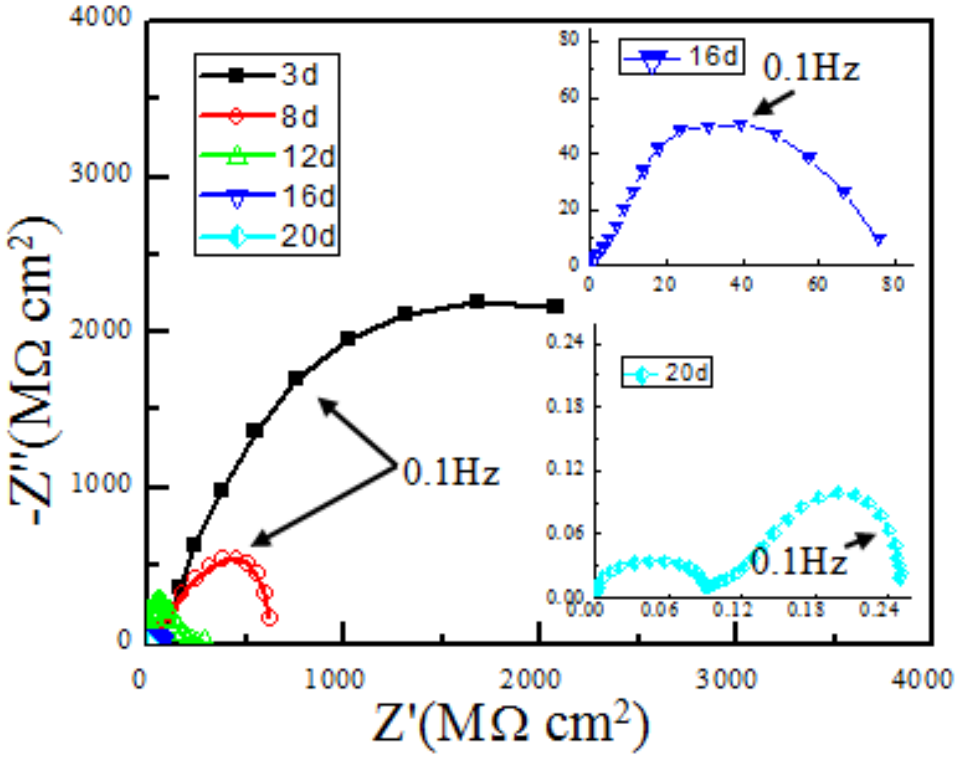

Figure 6. Nyquist plots for coated plates after NSS test.

The Nyquist plots, after various periods of NSS testing, are shown in Figure 6. In contrast to EIS obtained from constant voltage testing, the arc only reduces in size with increasing test time. Up to 16 d, only one arc is observed for a single curve, suggesting a single time constant is involved. At 20 d, a 2nd arc appears which indicates the substrate has been corroded. It is at this time that the white rust product was observed on the topcoat surface. This was followed by the "red rust" of substrate corrosion at 24 d.

Based on the equivalent circuits from Figure 4, the exact value of each component was calculated and listed in Table 3. The logarithm of $CPE_{coating}$ and R_c are plotted as a function of elapsed time and shown in Figure 7.

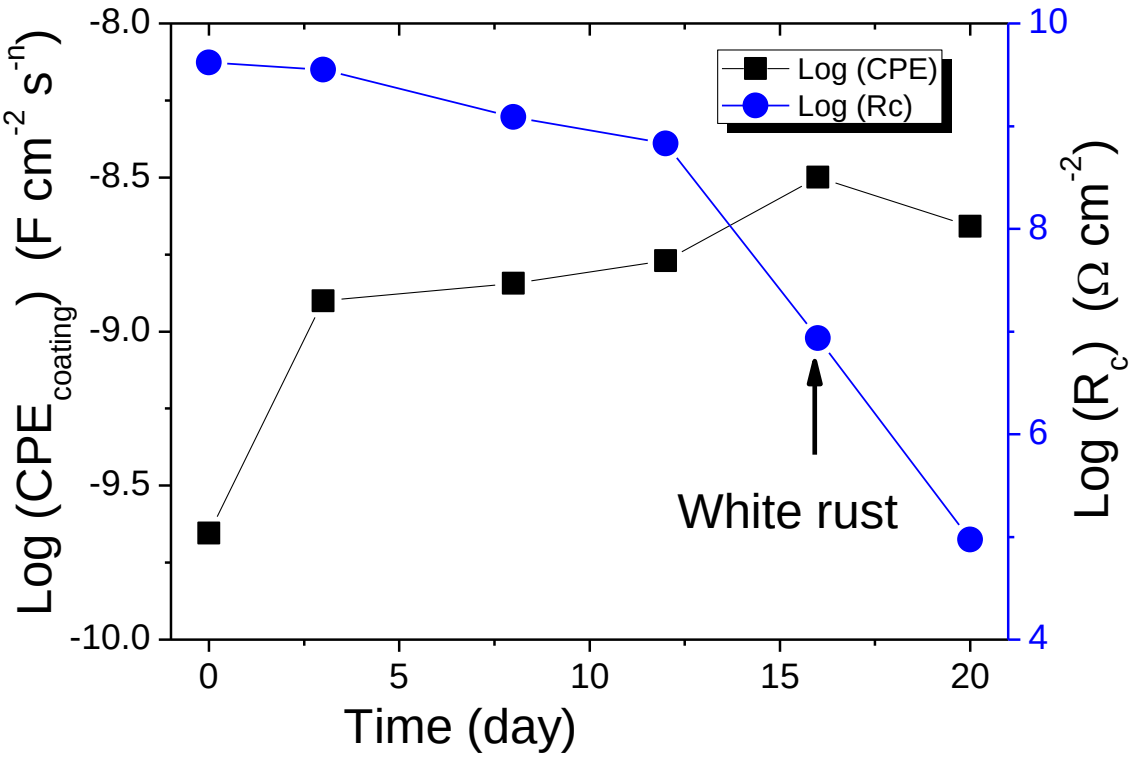

Figure 7. Time dependence of logarithm resistance $CPE_{coating}$ and R_c of NSS test.

Table 3. EIS data simulation after NSS test

Time (day)	$CPE_{coating}$ ($F\ cm^{-2}\ s^{-n}$)	R_c ($\Omega\ cm^{-2}$)	CPE_{DL} ($F\ cm^{-2}\ s^{-n}$)	R_{ct} ($\Omega\ cm^{-2}$)
0	2.218×10^{-10}	4.169×10^{9}	/	/
3	1.258×10^{-9}	3.548×10^{9}	/	/
8	1.435×10^{-9}	1.231×10^{9}	/	/
12	1.698×10^{-9}	6.767×10^{8}	/	/
16	3.167×10^{-9}	8.589×10^{6}	1.583×10^{-7}	7.477×10^{7}
20	2.198×10^{-9}	9.443×10^{4}	1.755×10^{-6}	1.76×10^{5}

As occurred with the constant voltage test, the water uptake into the coating during NSS is responsible for the increase in the coating capacitance and the decrease in the coating resistance R_c. The $CPE_{coating}$ remains relatively stable during the remaining time of the NSS test, except for an increase at 16 d. This is the time the white rust is observed on the surface, and this corrosion product

increases the dielectric constant of the coating. Prior to the "white rust" appearing on the surface, the R_c value, shows a rapid decrease, indicating the electrolyte has fully penetrated through the topcoat.

4. DISCUSSION

4.1 Reactions occurring in the constant voltage and NSS tests

The R_c value for the constant voltage test reaches the maximum 1.45×10^{10} Ω cm^{-2} at 14 h and then it fluctuates between 14 and 70 h, as shown in Figure 5. Using a constant voltage of 3.5 V, the corrosive media penetrates rapidly through the topcoat. Once through the topcoat, zinc from ZRP is rapidly oxidized. Generally the zinc oxidized species includes: ZnO, $Zn(OH)_2$, $Zn(HCO_3)_2$, $ZnCO_3$ and $3Zn(OH)_2{\cdot}3ZnCO_3$. The reaction is sufficiently rapid to prevent the oxidized species passing through the pores of the top layer. This results in the pores becoming blocked by the oxidized zinc species, which results in an increase in the R_c value. It takes some time to clear the penetration path for corrosive species, but once cleared the oxidation of zinc begins again and the process repeats. The aggressive nature of this process is likely the cause of any oxidized zinc species appearing on the surface, and this process explains the R_c fluctuation during 14-70 h during constant voltage test prior to dynamic equilibrium ~~is~~ being achieved.

The significant volume expansion results in the raised surface and cracking as shown by the SEM image in Figure 1(b). This allows the electrolyte to penetrate to the substrate and oxidation of the steel substrate begins and subsequently the "red rust" appears on the surface. The corresponding current during the constant voltage test further confirmed the variation in the trend shown by the EIS test.

In the case of NSS test, a much longer time was required for the corrosive species to penetrate through the top coat. The reactions involved in the oxidation of zinc are not as vigorous as that in constant voltage test as shown by the relatively small area of raised surface (see Figure 1(f)). Also seen in Figure 1(f) and (g) are cracks in the surface of the NSS sample that allow the diffusion of the oxidized zinc species and these allow the R_c to steadily decrease in contrast to the constant voltage test.

4.2 Constant Voltage vs. NSS

Previously, researchers had widely utilizied salt spray and EIS to evaluate the performance of corrosion resistant coatings. Yang [28] studied the anticorrosive properties of hexamethylene diisocyanate microcapsule-based self-healing coatings. By salt spray test of scratched samples, it revealed that the thicker coatings with larger microcapsules at 10 wt.% demonstrated the best anticorrosion behavior, and the kinetics of self-healing process was further characterized by EIS measurement. Similarly, Ramezanzadeh [29] studied the corrosion resistance enhancement by Cr_2O_3 nanoparticles modified with 3-amino propyl trimethoxy silane in the polyurethane coating matrix. The results of EIS, salt spray and SEM showed that 3-amino propyl trimethoxy silane could achieve proper dispersion and increment compatibility, and addition of surface modified nanoparticles caused significant increase in the corrosion resistance of the polyurethane coating. Furthermore, Li Yantao [30]

studied the zinc-aluminum coatings behavior and protection mechanism by salt spray test and EIS. Influence of the Cerium Concentration was studied on the Corrosion Performance of Ce-doped Silica Hybrid Coatings on Hot Dip Galvanized Steel Substrates as well by the same techniques [31].

However, little publications had studied the novel corrosion assessment technique correlation with salt spray. Therefore, we further compare the EIS results of initial period and rust pint of both the constant voltage and NSS tests, in order to establish the correlation. In Figure 8 are shown the Nyquist plots comparison for two techniques at the initial period and rust point. In Figure 8(a) the plots of the initial periods of NSS (3 d) and constant voltage (24 h) are displayed. The curves are of the same magnitude and show the same trend, i.e. a single time constant, indicating the corrosive media permeation process are similar. In Figure 8(b) are shown the Nyquist plots corresponding to the rust point; constant voltage (90 h) and NSS (24 d). The arcs have a similar magnitude and shape, implying a close corrosion state.

It is noted that it takes just 90 h for the constant voltage test to reach the similar corrosion state as the NSS achieves in 20 days showing a significant increase in the acceleration rate of the corrosion test. In the constant voltage test, maintaining the uniform electric field is crucial, to detect the less corrosion resistant area, so a stable and suitable counter electrode is required. However, it is hard to design the counter electrode for test pieces with complex geometries. Therefore, unless otherwise specified, constant voltage test is only applicable to flat surfaces.

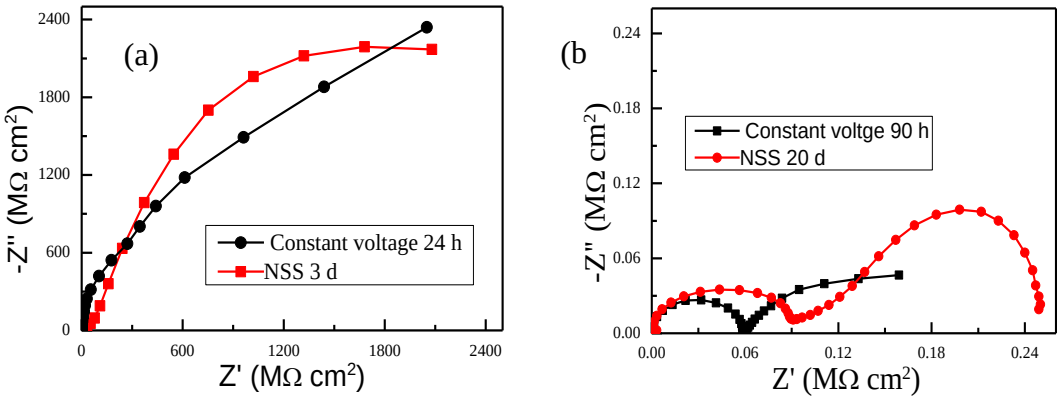

Figure 8. Comparison of Nyquist plots between constant voltage and NSS test. (a) Initial period; (b) red rust period

5. CONCLUSIONS

A novel corrosive property evaluation method is proposed in the form of a constant voltage test. EIS testing was used to allow a comparison between this new test method and the well recognized NSS test.

During constant voltage test at 3.5 V vs. graphite, the EIS shows a single semicircle from 0 to 70 h, and the second semicircle appeared at 80 h, indicating the onset of substrate corrosion. The coating resistance decreases after 8 h and then fluctuates between 14 to 70 h, reaching a maximum of

1.45×10^{10} Ω cm^{-2} at 14 h. Once the corrosive species penetrate through the topcoat, zinc is oxidized rapidly from ZRP. The pores in the topcoat become blocked by the zinc oxidized species, which increases the R_c value. It then takes some time to clear the penetration path for corrosive species before the oxidation of zinc continues. This process explains the fluctuation of R_c during 14-70 h period of constant voltage testing. As soon as the oxidation of the substrate begins, the "red rust" appears on the topcoat surface. Meanwhile, due to the significant volume expansion, cracks also appear on the coating surface. The corresponding current during the constant voltage test further confirmed the variation trend observed by EIS test.

In the case of NSS test, a substantially longer period of time is required for the corrosive species to penetrate through the top coat. The reaction of zinc oxidation was not as vigorous as that in constant voltage test and the corrosive species diffusion path was not totally blocked by the zinc oxidized species, consequently, in contrast to the constant voltage test, R_c decreased steadily.

Overall it takes just 90 h for constant voltage to reach a similar corrosion state that takes NSS 20 days. The acceleration rate of the corrosion test is significant. However, because constant voltage testing requires a stable counter electrode to keep a constant electric field over the entire surface, it is not applicable for test pieces with complicated geometries.

ACKNOWLEDGEMENTS

This work was supported by the National Environmental Corrosion Platform (NECP), and Shenzhen Peacock Plan Program (KQCX20140521144358003), Innovation Institutions Construction Projects of Nanshan District, Shenzhen (KC2015ZDYF0009A), International Collaboration Program of Shenzhen (GJHZ20130411141529167), Fundamental research plan of Shenzhen (JCYJ20140417172417144).

References

1. I. Sekine, *Prog. Org. Coat*. 31 (1997) 73.
2. C. Zhou, X. Lu, Z. Xin, J. Liu, Y. Zhang, *Corros. Sci*. 80 (2014) 269.
3. ISO 12944-1:1998 (E), Paints and Varnishes-Corrosion Protection of Steel Structures by Protective Paint Systems 1st edn., 1998.
4. R.G. Hua, S. Zhanga, J.F. Bua, C.J. Lina, G.L. Song, *Prog. Org. Coat.* 73 (2012) 129-141.
5. Y. Gonza´lez-Garcı´a, S. Gonza´lez, R.M. Souto, *Corros. Sci*. 49 (2007) 3514.
6. M. Liu, X. Mao, H. Zhu, A. Lin, D. Wang, *Corros. Sci.* 75 (2013) 106.
7. M. Orazem, B. Tribollet, Electrochemical Impedance Spectroscopy, Wiley-Interscience, New Jersey 2008.
8. S. Subrahmanya, P. Bajaj, B. P. Mallik, *Electrochim. Acta* 55 (2010) 5129.
9. X. Liu, J. Xiong, Y. Lv, Y. Zuo, *Prog. Org. Coat*. 64 (2009) 497.
10. F.L. Floyd, S. Avudaiappan, J. Gibson, B. Mehta, P. Smith, T. Provder, J. Escarsega, *Prog. Org. Coat.* 66 (2009) 8.
11. S. Shreepathi, A.K. Guin, S.M. Naik, M.R.Vattipalli, *J. Coat. Technol. Res*. 8 (2011) 191.
12. C. Hall, S. Field, K. Zuber, P. Murphy, D. Evans, *Corros. Sci*. 69 (2013) 406.
13. ASTM B 117-03, Standard Practice for Operating Salt Spray (Fog) Apparatus. ASTM Standards, 2003.
14. ASTM G 85-02, Standard Practice for Modified Salt Spray (Fog) Testing. ASTM Standards, 2003.
15. ASTM D 5894-05, Standard Practice for Cyclic Salt Fog/UV Exposure of Painted Metal

(Alternating Exposures in a Fog/Dry Cabinet and a UV/Condensation Cabinet). ASTM Standards, 2005.
16. B.R. Appleman, *J. Coat. Tech*. 62 (1990) 57.
17. D.Mills, S.Jamali, M.T. Tobiszewski, *Prog. Org. Coat*. 74 (2012) 385.
18. G.P. Bierwagena, L. He, J. Li, L. Ellingson, D.E. Tallman, *Prog. Org. Coat*. 39 (2000) 67.
19. C. H. Tsai, F. Mansfeld, *Corrosion*, 49 (1993) 726.
20. V. Barranco, S. Feliu Jr., S. Feliu, *Corros. Sci*. 46 (2004) 2203.
21. G. Luckeneder, M. Fleischanderl, T. Steck, K.H. Stellnberger, J. Faderl, S. Schuerz, G. Mor, BHM Berg-und Hüttenmännische Monatshefte 157 (2012) 121.
22. H. Marchebois, C. Savall, J. Bernard, S. Touzain, *Electrochim. Acta* 49 (2004) 2945.
23. H. Marchebois, S. Touzain, S. Joiret, J. Bernard, C. Savall, *Prog. Org. Coat.* 45 (2002) 415.
24. H. Marchebois, S. Joiret, C. Savall, J. Bernard, S. Touzain, *Surf. Coat. Technol*. 157 (2002) 151.
25. J.R. Vilche, E.C. Bucharsky, C.A. Giudice, *Corros. Sci*. 44 (2002) 1287.
26. A. Meroufel, S. Touzain, *Prog. Org. Coat*. 59 (2007) 197.
27. A. R. Marder, *Prog. Mater. Sci*. 45 (2000) 191.
28. M. Huang, J. Yang, *Prog. Org. Coat*. 77 (2014) 168.
29. M.J. Palimi, M. Rostami, M. Mahdavian, B. Ramezanzadeh, *Prog. Org. Coat*. 77 (2014) 1935.
30. Li Yantao, Yang Lihui, Li Xiao, Liu Jianguo, Hou Baorong, *Int. J. Electrochem. Sci*. 8 (2013) 9886.
31. R. Zandi Z, K. Verbeken, A. Adriaens, *Int. J. Electrochem. Sci*. 8 (2013) 548.